Available online at www.sciencedirect.com
ScienceDirect
Dyes and Pigments 75 (2007) 130–135
DYES and PIGMENTS
www.elsevier.com/locate/dyepig

Adsorption kinetic, thermodynamic and desorption studies of C.I. Reactive Black 5 on a novel photoassisted Fenton catalyst

Chan-Li Hsueh, Yu-Wen Lu, Chil-Chang Hung, Yao-Hui Huang*, Chuh-Yung Chen

Department of Chemical Engineering, National Cheng Kung University, Tainan City 701, Taiwan

Received 28 March 2006; accepted 22 May 2006
Available online 13 July 2006

Abstract

An activated alumina-supported iron oxide-composite (denoted as FeAA-25) was utilized successfully as a catalyst for the heterogeneous photoassisted Fenton degradation of the azo dye C.I. Reactive Black 5 (RB5) at a pH of 7.0 in our previous study. In this work, the adsorption and desorption behaviours of RB5 on FeAA-25 were studied. Adsorption thermodynamics of RB5 on FeAA-25 were studied at 288, 303 and 318 K and the thermodynamic parameters, such as equilibrium constant (K_0), standard free energy changes (ΔG^0), standard enthalpy change (ΔH^0) and standard entropy change (ΔS^0) have been obtained. A pseudo-second-order rate model was employed to describe the kinetic adsorption processes. Additionally, desorption studies revealed that RB5 can be easily removed from FeAA-25 by altering the pH of the solution using NaOH. The mechanism of the RB5 adsorption onto FeAA-25 at neutral pH 7.0 will be established through this study.

Keywords: Adsorption; Iron oxide; Thermodynamic; Kinetics; Reactive Black 5; Desorption

1. Introduction

Dye effluents, discharged from the dyestuff manufacturing, dyeing, printing, and textile industries, may contain chemicals that exhibit toxic effects toward microbial populations and can be toxic and/or carcinogenic to mammals. Conventional methods for the removal of dyes in effluents include physical, chemical, and biological processes [1]. Unfortunately, most azo dye compounds are resistant to bacterial activity and biological treatment alone will take a long time to be effective. Therefore, alternative technology must be developed to help solve the problem.

Adsorption and advanced oxidation processes (AOPs) have been among the promising processes for removing hazardous and environmentally undesirable chemicals. The adsorption process is one of the most widely used methods for the removal of pollutants from water with advantages of high treatment efficiency and no contaminative by-product released into treated water. However, the adsorption process transfers pollutants from one phase to another rather than eliminating them from environment and, thus, will cause secondary pollution. When adsorbents are used to adsorb toxic compounds or decontaminate effluents, they become hazardous wastes that should be treated or disposed off properly. A more satisfactory method of pollution abatement is by mineralization of pollutants.

Advanced oxidation processes refer to the remediation processes that generate the highly reactive hydroxyl radical ($^{\bullet}OH$) to degrade organic pollutants [2,3]. AOPs have attracted wide interests in wastewater treatment since 1990s [4–7]. Among AOPs, one of the most important processes used to generate $^{\bullet}OH$ is $Fe^{2+}/H_2O_2/UV$ system, where the catalyst of ferrous ions is dissolved in water so it is called homogeneous photo-Fenton process. In this system, Fe^{2+} in solution functions as a homogeneous catalyst. However, the large volume of the Fe(III)-iron sludge following a Fenton reaction is a serious problem because removing Fe(III)-iron sludge at the end of the treatment by precipitation is rather expensive. This drawback limits the further application of homogeneous photo-Fenton process in wastewater treatment.

* Corresponding author. Tel.: +886 6 2757575/62636; fax: +886 6 2344496.
E-mail address: yhhuang@ccmail.ncku.edu.tw (Y.-H. Huang).

0143-7208/$ - see front matter © 2006 Elsevier Ltd. All rights reserved.
doi:10.1016/j.dyepig.2006.05.020

Thus, it appears beneficial to combine adsorption with advanced oxidation in a water treatment system. Through this process, the mineralization of organic contaminants and the regeneration of adsorbent occur at the same time. Recently, there is a growing interest in low-cost, high-surface area materials, especially metal oxides, and their unique applications, including adsorption and chemical catalysis. It is well known that the smaller the particles are, the better their properties of adsorption and catalysis, but the solid–liquid separation is more difficult. Iron oxide have a relatively high-surface area and charge; many researchers have applied iron oxide (i.e., maghemite, hematite and goethite) as adsorbent for the treatment of heavy metals and organic compounds from wastewater [8–10]. Most iron oxides are available only as fine powders or are generated in aqueous suspensions as hydroxide floc or gel. In such forms, these oxides retain their desirable adsorptive properties for the trace metals and organic compounds, but they are limited to application because of the difficulty of solid–liquid separation. Recently, some researchers have developed techniques for coating iron oxide onto porous solid as the catalyst, which is called the heterogeneous catalyst because it dose not dissolve in water [11–16]. However, those materials have two major shortcomings that considerably constrain their practical usefulness on a large scale. The first is that the Nafion film is too expensive for practical use [11–13]. The second is that the catalysts are still limited to the acidic pH range and the optimum solution pH is 3.0 [14–16].

This study explores an activated alumina-supported iron oxide-composite material (FeAA-25), which is a by-product of the FBR–Fenton reaction [17,18], used in the treatment of the bioeffluent of tannery wastewater from a dyeing/finishing plant in Taiwan. The FeAA-25 has successfully been used as heterogeneous photoassisted Fenton catalyst for the degradation of RB5 at neutral pH 7.0 in our previous study [19]. In the meantime, the mechanism for catalyst in a heterogeneous photoassisted Fenton reaction is proposed. The RB5 can be adsorbed well on the surface of FeAA-25 at neutral pH 7.0 which is the key factor in the mechanism. Because of the photolysis of Fe(III)–dye chelates which are formed during photo-oxidation can produce organic radicals resulting in an enhanced rate of destruction of dye molecules [20].

$$\text{Fe(III)–dye} + h\nu \rightarrow \text{Fe}^{2+} + \text{dye}^{\bullet} \quad (1)$$

Thus, in this paper, we will investigate the thermodynamics and kinetics of the adsorption of C.I. Reactive Black 5 onto FeAA-25 at pH 7.0, in order to obtain the thermodynamic parameters, to establish the adsorption rate equation and to improve our understanding of the mechanism of heterogeneous photo-oxidation in the environment.

2. Materials and methods

2.1. Materials

The FeAA-25 was prepared by FBR–Fenton reaction and its properties are described in our previous publications in detail [19]. C.I. Reactive Black 5 (RB5) was purchased from Aldrich Chemical Company (Amherst, NY, USA) and had an M_r of 991.82; the structure of RB5 is presented below. Deionized and doubly distilled water were used throughout this investigation. By dissolving RB5 in deionized water, we obtained the dye containing stock solution (1000 mg l^{-1}), which was further diluted to the required concentrations before being used.

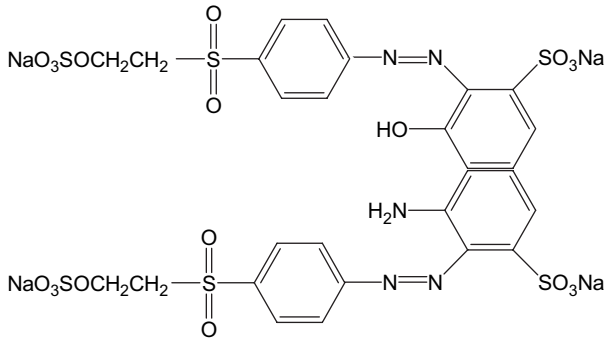

C.I. Reactive Black 5 (RB5)

2.2. Analytical measurements

The RB5 spectrum showed an absorption peak at 597 nm. Therefore, the concentration of RB5 solution was determined from the absorption intensity at 597 nm using a UV–vis spectrometer (Jasco Model 7850). Before the measurement was made, a calibration curve was plotted using the standard RB5 with known concentrations.

2.3. Batch experimental programme

To study the effect of important parameters batch experiments were conducted. For each experimental run, 100 ml of dye of known concentration, pH and the known amount of the FeAA-25 were taken in a 150 ml stoppered conical flask. This mixture was agitated at a temperature controlled by shaking water bath at a constant speed of 100 revolutions per minute (rpm). Samples were withdrawn at appropriate time intervals and analyzed for dye concentration spectrophotometrically using UV-spectrophotometer. Experiments were controlled at pH 7.0 ± 0.05 by the addition of dilute HCI or NaOH solutions.

Adsorption kinetic samples were prepared by adding 0.5 g of FeAA-25 into 100 ml solution (pH 7.0), and the RB5 concentration was 20, 40 and 60 mg l^{-1}, separately, at 303 K. The RB5 adsorption amount at time t, q_t (mg g^{-1}), was calculated by

$$q_t = \frac{(C_0 - C_t)V}{W}, \quad (2)$$

where C_0 and C_t are the RB5 concentrations contained in the original solution and after time t, respectively; V is the volume of the solution and W represents the weight of the FeAA-25 used.

To evaluate the thermodynamic properties, we first prepared various solutions with initial RB5 concentrations ranging from

20 to 200 mg l^{-1} (20 mg l^{-1} interval, 100 ml, pH 7) and from 250 to 500 mg l^{-1} (50 mg l^{-1} interval, 100 ml, pH 7), and then added 0.5 g FeAA-25 to each solution. These samples were then mounted on a shaking water bath and shaken continuously for 192 h at 288, 303 and 318 K, respectively. The differences between the initial and the equilibrium RB5 concentrations determine the amount of RB5 adsorbed by FeAA-25.

In order to investigate the desorption capacity of RB5 from FeAA-25, 0.5 g FeAA-25 were introduced into 100 ml solution whose initial RB5 concentration is 60 mg l^{-1} and pH is 7.0. As the adsorption reaches equilibrium, the RB5 concentration of the solution was measured, and then the solution pH values of the solution were adjusted, from 7.0 to 12.0, using NaOH solutions. After the solutions reach equilibrium, the RB5 concentrations were remeasured and the desorption results were then obtained.

3. Results and discussion

3.1. Adsorption kinetic study

Adsorption kinetics, demonstrating the solute uptake rate, is one of the most important characteristics which represents the adsorption efficiency of FeAA-25 and therefore, determines their potential applications. According to Fig. 1, the RB5 adsorption rates increase dramatically in the first 300 min for various initial concentrations, and they reach equilibrium gradually at 600, 720 and 960 min, corresponding to RB5 initial concentrations of 20, 40 and 60 mg l^{-1}, respectively. To analyze the adsorption rate of RB5 onto the FeAA-25, the pseudo-second-order rate equation was evaluated based on the experimental data [21].

$$\frac{t}{q_t} = \frac{1}{2K' q_e^2} + \frac{t}{q_e}, \tag{3}$$

where K' stands for the pseudo-second-order rate constant of adsorption (g mg^{-1} min^{-1}). Linear plot feature of t/q_t vs. t

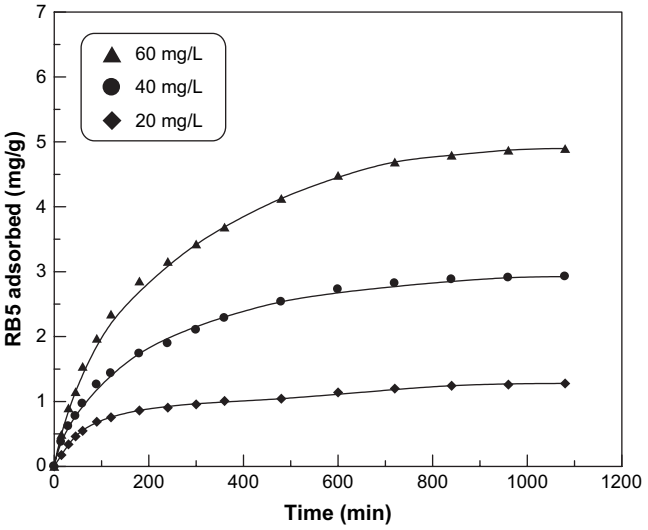

Fig. 1. Effect of contact time on RB5 adsorption rate for different concentrations (pH = 7.0, at 303 K).

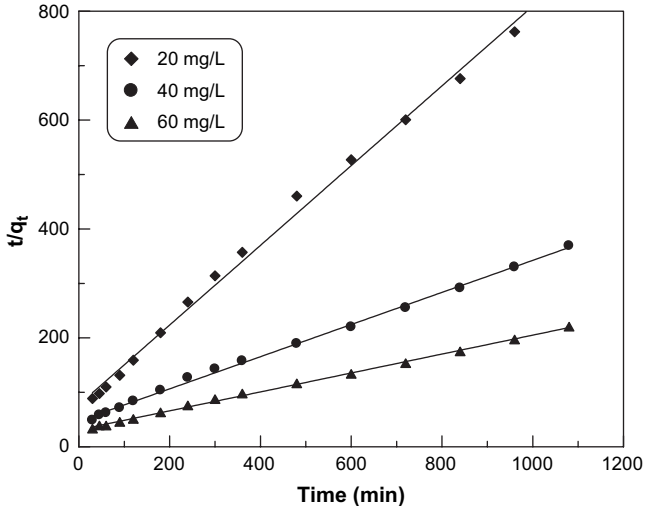

Fig. 2. Test of pseudo-second-order rate equation for adsorption of different concentrations of RB5 by FeAA-25 (pH = 7.0, at 303 K).

(Fig. 2) was achieved and the K' values calculated from the slopes and intercepts were summarized in Table 1. The correlation coefficients of the pseudo-second-order rate model for the linear plots are very close to 1, thus suggesting that kinetic adsorption can be described by the pseudo-second-order rate equation.

3.2. Adsorption equilibrium study

Fig. 3 shows the adsorption isotherms of RB5 on FeAA-25 at 288, 303 and 318 K. These data could be approximated by the Freundlich isotherm model, which depicts the relationship between the amount of RB5 adsorbed by per unit mass of FeAA-25 (q_e, mg g^{-1}) and the equilibrium concentration of RB5 (C_e, mg l^{-1}) in solution:

$$q_e = K_F C_e^{1/n}, \tag{4}$$

where K_F and n are Freundlich constants related to the adsorption capacity and adsorption intensity, respectively. The Freundlich equation is applicable to highly heterogeneous surfaces, and an adsorption isotherm lacking a plateau indicates a multi-layer adsorption [22]. The parameter K_F refers to the relative adsorption capacity, i.e., FeAA-25 exhibits higher RB5 adsorption capacity at 318 K than at 288 K, according to the K_F data shown in Table 2. Based on Eq. (4), we obtained a straight line when plotting ln q_e vs. ln C_e (Fig. 4). The constants, K_F and n, are then defined by the intercepts and slopes of the line, respectively. It appears that the Freundlich model agrees well with our experimental data

Table 1
Kinetic parameters of RB5 adsorbed on FeAA-25 at different initial RB5 concentrations

Initial RB5 concentration (mg l^{-1})	Pseudo-second order		
	q_e	K'	R^2
20	1.37	0.00347	0.9955
40	3.39	0.00092	0.9981
60	5.75	0.00048	0.9984

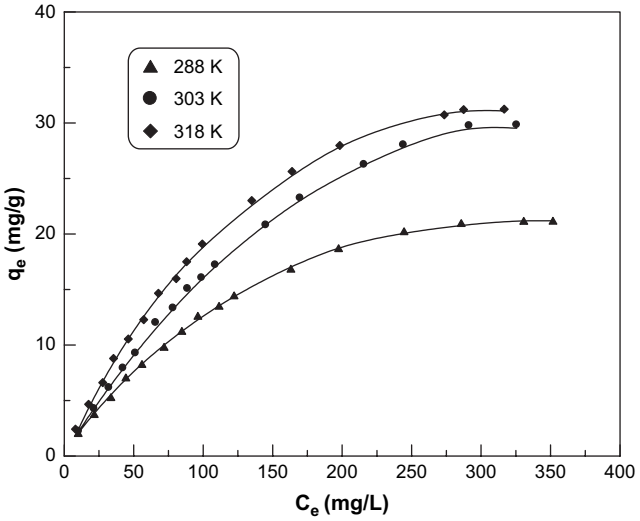

Fig. 3. Adsorption isotherms of RB5 onto FeAA-25 at different temperatures.

(Table 2), with the correlation coefficient values being close to 1 at different temperatures. The RB5 adsorption capacity increases with the rise of temperatures, indicating an endothermic reaction. Thermodynamic parameters can be calculated from the variation of the thermodynamic equilibrium constant K_0 with the change in temperature [23]. For adsorption reactions, K_0 is defined as follows:

$$K_0 = \frac{a_s}{a_e} = \frac{v_s}{v_e}\frac{C_s}{C_e} \tag{5}$$

where a_s is the activity of adsorbed RB5, a_e is the activity of the RB5 in solution at equilibrium, C_s is the amount of RB5 adsorbed by per mass of FeAA-25 (mmol g^{-1}) and C_e is the RB5 concentration in solution at equilibrium (mmol ml^{-1}), v_s is the activity coefficient of the adsorbed RB5 and v_e is the activity coefficient of the RB5 in solution at equilibrium. As the RB5 concentration in the solution decreases and approaches zero, K_0 can be obtained by plotting $\ln(C_s/C_e)$ vs. C_s (Fig. 5) and extrapolating C_s to zero [23]. The straight line obtained is fitted to the points based on a least-squares analysis. Its intercept with the vertical axis gives the values of K_0. The adsorption standard free energy changes (ΔG^0) can be calculated according to

$$\Delta G^0 = -RT\ln K_0, \tag{6}$$

where R is the universal gas constant (1.987 cal deg^{-1} mol^{-1}) and T is the temperature in Kelvin. The average standard enthalpy change (ΔH^0) is obtained from Van't Hoff equation

Table 2
Parameters of Freundlich adsorption isotherm models for RB5 on FeAA-25

Temperature (K)	Freundlich adsorption isotherm model		
	K_F	n	R^2
288	0.341	1.271	0.9984
303	0.288	1.136	0.9988
318	0.440	1.212	0.9984

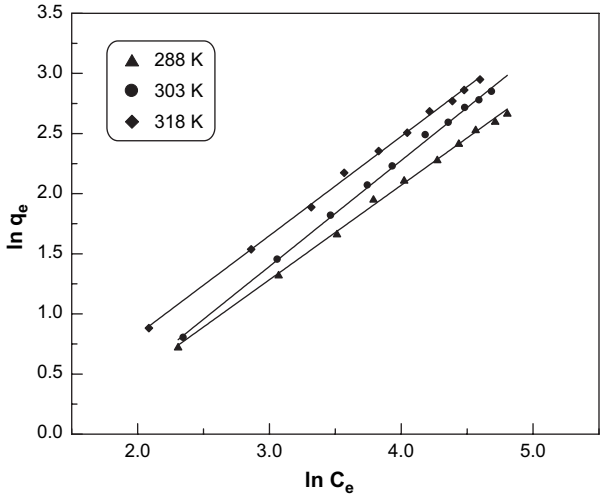

Fig. 4. Linearized Freundlich isotherms for RB5 adsorption by the FeAA-25 at different temperatures.

$$\ln K_0(T_3) - \ln K_0(T_1) = \frac{-\Delta H^0}{R}\left(\frac{1}{T_3} - \frac{1}{T_1}\right), \tag{7}$$

where T_3 and T_1 are two different temperatures. The standard entropy change (ΔS^0) can be obtained by the following equation

$$\Delta S^0 = -\frac{\Delta G^0 - \Delta H^0}{T}, \tag{8}$$

The thermodynamic parameters are listed in Table 3. A positive standard enthalpy change suggests that the interaction of RB5 adsorbed by FeAA-25 is endothermic, which is supported by the increasing adsorption of RB5 with the increase in temperature; a negative adsorption standard free energy change and a positive standard entropy change indicate that the adsorption reaction is a spontaneous process [23]. The positive standard entropy change may be due to the release of water molecule produced by ion exchange reaction between

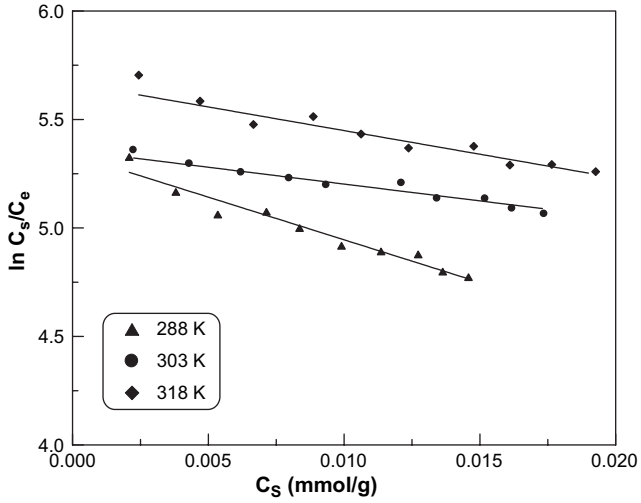

Fig. 5. Plots of ln C_s/C_e vs. C_s at various temperatures.

Table 3
Values of various thermodynamic parameters for adsorption of RB5 on FeAA-25

Thermodynamic constant	Temperature (K)		
	288	303	318
k_0	5.339	5.378	5.705
ΔG^0(× 1000 cal mol^{-1})	−0.959	−1.013	−1.100
ΔH^0(× 1000 cal mol^{-1})	0.402	0.402	0.402
ΔS^0(cal mol^{-1} K^{-1})	4.724	4.670	4.724

the adsorbate and the functional groups on the surfaces of FeAA-25.

3.3. Desorption in response to the pH value and repetitive cycles of adsorption and desorption

After the adsorption of RB5 on FeAA-25 was equilibrated desorption was carried out by altering the pH values of the solution using NaOH. Fig. 6 shows the changes in the degree of desorption determined from the adsorbed amount and the desorbed amount with the equilibrium pH value. The degree of desorption increased with an increase in the equilibrium pH value, and the quantities of RB5 adsorbed (ca. 100%) were desorbed at the equilibrium, pH 12, regardless of the RB5 used here. These results show that the RB5 adsorbed by FeAA-25 can easily be desorbed by altering the pH values of the solution using NaOH.

On the basis of the results for the pH dependence of adsorption and desorption of RB5 presented in Fig. 6, the reusability of FeAA-25 was examined by the alternating repetition of the cyclic process of adsorption at the initial pH value of 7.0 and desorption at the equilibrium pH 12. Fig. 7 shows three successive RB5 adsorption–desorption cyclic processes in response to the pH change in the medium. After the first desorption process, RB5 adsorbed on the FeAA-25 to the near adsorbed amount as that of the first adsorption process. The

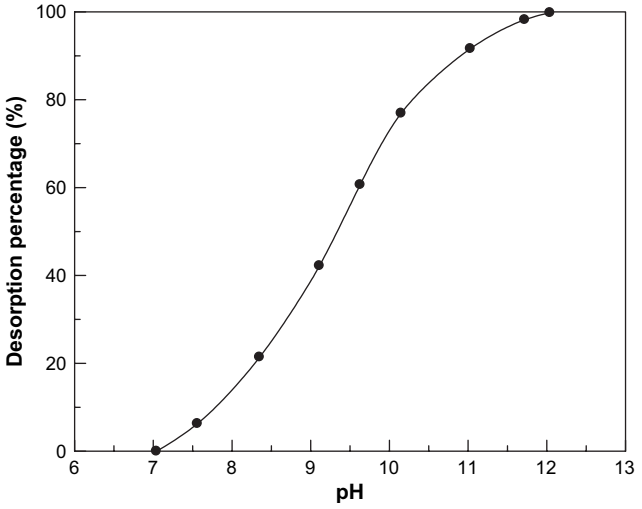

Fig. 6. Desorption of RB5 from FeAA-25 by adjusting the pH values of the solution using NaOH solution. The adsorption of RB5 was carried out at pH 7.0 before the desorption experiments.

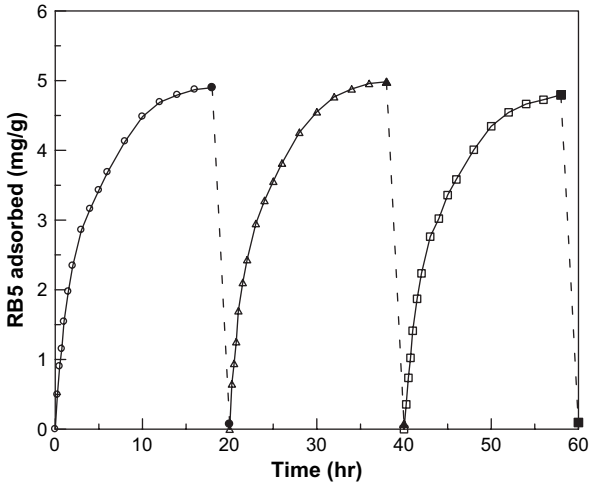

Fig. 7. Alternately repeated cyclic process of adsorption at the initial pH value 7.0 (open symbols) and desorption at the pH value 12.0 (shaded symbols) for FeAA-25 at 303 K: (○,●) first run, (△,▲) second run, and (□,■) third run.

physicochemical properties obtained for the repeated cyclic processes of adsorption and desorption of RB5 are summarized in Table 4. The amounts of adsorbed and desorbed RB5 were almost equivalent, and the kinetic constants of adsorption stayed unchanged in each adsorption process. These results indicate that the FeAA-25 can endure several cycles of the adsorption and desorption processes in response to the pH change without considerable fatigue.

4. Conclusions

A positive value of the standard enthalpy change suggests that the interaction of RB5 when adsorbed by FeAA-25 is endothermic. The negative adsorption standard free energy changes and positive standard entropy changes indicate that the adsorption reaction is a spontaneous process. The kinetic adsorption process can be well described by the pseudo-second-order rate model. RB5 can be easily desorbed from FeAA-25 by adjusting the solution pH values. By this study, the understanding of the mechanism of heterogeneous photo-oxidation at neutral pH in the environment can be enhanced.

Table 4
Physicochemical properties of alternately repeated cycle process of adsorption at the pH value of 7.0 and desorption at the pH value of 12.0 of RB5 for FeAA-25

	First run	Second run	Third run
Adsorbed amount (mg g^{-1})	4.90	4.96	4.80
Degree of desorption (%)	98.6	98.4	98.0
Kinetic constant of adsorption × 10^6 (g mg^{-1} min^{-1})	484	474	472

Acknowledgements

The authors thank the National Science Council of the Republic of China for financially supporting this NSC94-2211-E-006-032.

References

[1] Wang S, Li H, Longya X. Application of zeolite MCM-22 for basic dye removal from wastewater. J Colloid Interface Sci 2006;295:71–8.
[2] Bahorsky MS. Textiles. Water Environ Res 1997;69:658–64.
[3] Cha DK, Song JS, Sarr D, Kim BJ. Hazardous waste treatment technologies. Water Environ Res 1996;68:575–86.
[4] Kang SF, Liao CH, Chen MC. Pre-oxidation and coagulation of textile wastewater by the Fenton process. Chemosphere 2002;46:923–8.
[5] Theruvathu JA, Aravindakumar CT, Flyunt R, Sonntag JV, Sonntag CV. Fenton chemistry of 1,3-dimethyluracil. J Am Chem Soc 2001;123: 9007–14.
[6] Lee BD, Hosomi M. Fenton oxidation of ethanol-washed distillation-concentrated benzo(A)pyrene: reaction product identification and biodegradability. Water Res 2001;35:2314–9.
[7] Ruppert G, Bauer R, Heisler G, Novalic S. Mineralization of cyclic organic water contaminants by the photo-Fenton reaction. Influence of structure and substituents. Chemosphere 1993;27:1339–47.
[8] Benjamin MM, Lecke JO. Multiple site adsorption of Cd, Cu, Zn, and Pb on amorphous iron oxyhydroxide. Colloid Interface Sci 1981;79:209–15.
[9] Gu B, Schmitt J, Chen Z, Liang L, McCarthy JF. Adsorption and desorption of nature organic matter on iron oxide: mechanisms and model. Environ Sci Technol 1994;28:38–46.
[10] Heijman SGJ, Paassen AM, Meer WGJ, Hopman R. Adsorption removal of natural organic matter during water treatment. Water Sci Technol 1999;40:183–90.
[11] Fernandez J, Bandara J, Lopez A, Buffar P, Kiwi J. Photoassisted Fenton degradation of nonbiodegradable azo dye (Orange II) in Fe-free solutions mediated by cation transfer membranes. Langmuir 1999;15:185–92.
[12] Fernandez J, Djananjeyan MR, Kiwi J, Senuma Y, Hilborn J. Evidence for Fenton photoassisted processes mediated by encapsulated Fe ions at biocompatible pH values. J Phys Chem 2000;104:5298–301.
[13] Djananjeyan MR, Kiwi J, Albers P, Enea O. Photo-assisted immobilized Fenton degradation up to pH 8 of azo dye Orange II mediated by Fe^{3+}/Nafion/glass fibers. Helv Chim Acta 2001;84:3433–5.
[14] Feng J, Hu X, Yue PL, Zhu HY, Lu GQ. Degradation of azo-dye Orange II by a photoassisted Fenton reaction using a novel composite of iron oxide and silicate nanoparticles as a catalyst. Ind Eng Chem Res 2003;42:2058–66.
[15] Feng J, Hu X, Yue PL, Zhu HY, Lu GQ. A novel laponite clay-based Fe nanocomposite and its photo-catalytic activity in photo-assisted degradation of Orange II. Chem Eng Sci 2003;58:679–85.
[16] Feng J, Hu X, Yue PL, Zhu HY, Lu GQ. Discoloration and mineralization of Reactive Red HE-3B by heterogeneous photo-Fenton reaction. Water Res 2003;37:3776–84.
[17] Chou S, Huang C, Huang YH. Effect of Fe^{2+} on catalytic oxidation in a fluidized bed reactor. Chemosphere 1999;39:1997–2006.
[18] Chou S, Huang C, Huang YH. Heterogeneous and homogeneous catalytic oxidation by supported γ-FeOOH in a fluidized-bed reactor: kinetic approach. Environ Sci Technol 2001;35:1247–50.
[19] Hsueh CL, Huang YH, Wang CC, Chen CY. Photoassisted Fenton degradation of nonbiodegradable azo-dye (Reactive Black 5) over a novel supported iron oxide catalyst at neutral pH. J Mol Catal A Chem 2006;245:78–86.
[20] Arslan I, Balcioglu IA. Degradation of commercial reactive dyestuffs by heterogenous and homogenous advanced oxidation processes: a comparative study. Dyes Pigments 1999;43:95–108.
[21] Ho YS, McKay G. Pseudo-second order model for sorption processes. Process Biochem 1999;34:451–65.
[22] Daifullah AAM, Girgis BS, Gad HMH. A study of the factors affecting the removal of humic acid by activated carbon prepared from biomass material. Colloid Surf A Physicochem Eng Asp 2004;235:1–10.
[23] Niwas R, Gupta U, Khan AA, Varshney KG. The adsorption of phosphamidon on the surface of styrene supported zirconium tungstophosphate: a thermodynamic study. Colloid Surf A Physicochem Eng Asp 2000;164:115–9.